Deep-Sea Research Part I 152 (2019) 103107

Contents lists available at ScienceDirect

Deep-Sea Research Part I

journal homepage: www.elsevier.com/locate/dsri

Origin and preservation of archaeal intact polar tetraether lipids in deeply buried sediments from the South China Sea

Weiyan Wu[a], Yang Xu[a], Suning Hou[b], Liang Dong[c], Haodong Liu[d], Huanye Wang[e], Weiguo Liu[e], Chuanlun Zhang[d,*]

[a] State Key Laboratory of Marine Geology, Tongji University, Shanghai, 200092, China
[b] Utrecht University, 3584CD, Utrecht, the Netherlands
[c] State Key Laboratory of Microbial Metabolism, School of Life Sciences and Biotechnology, Shanghai Jiao Tong University, Shanghai, 200240, China
[d] Shenzhen Key Laboratory of Marine Archaea Geo-Omics, Department of Ocean Science and Engineering, Southern University of Science and Technology, Shenzhen, 518055, China
[e] State Key Laboratory of Loess and Quaternary Geology, Institute of Earth Environment, Chinese Academy of Sciences, Xi'an, 710075, China

ARTICLE INFO

Keywords:
Archaeal lipids
GDGTs
TEX_{86}
Deep biosphere
South China Sea

ABSTRACT

Intact polar lipids-glycerol dibiphytanyl glycerol tetraethers (IPL-GDGTs) are assumed to be degraded to core lipids (CL) upon cell death, which thus can serve as markers for live archaea in marine deep biosphere. However, the degradation models of sedimentary IPL-GDGTs suggested that they are mainly fossil compounds and can be preserved over geological timescales. Here we investigated the CL- and IPL-GDGTs from deeply buried sediments (0.1–485 mbsf, ~7.3 Ma) in the South China Sea (SCS). The depth profiles of IPL-GDGT concentrations paralleled those of CL-GDGTs. The sea surface temperatures (SST) derived from CL- and IPL-TEX_{86} ranged 23.1–28.8 °C and 22–33.3 °C, respectively. They are close to the SST in the SCS, suggesting that CL- and IPL-GDGTs mostly originate from pelagic archaea. The composition and distribution of the IPL-GDGTs differed among the polar headgroups. Hexose-phosphohexose (HPH)-GDGTs were dominated by GDGT-0, monohexose (1G)-GDGTs were mainly composed of GDGT-0 and crenarchaeol, and dihexose (2G)-GDGTs consist primarily of GDGT-2 and crenarchaeol isomer. The compositions of HPH-, 1G- and 2G-GDGTs are similar to those in previously studied water column samples, supporting that sedimentary IPL-GDGTs predominantly derive from the water column. HPH-GDGT abundances fast declined to be undetectable at ~31 mbsf (~0.6 Ma) while 1G- and 2G-GDGTs dominated the deeply buried sediments, indicating that GDGTs with glycosidic headgroups are better preserved versus GDGTs with phosphorous headgroups over geological timescales. Our results demonstrate that IPL-GDGTs, especially glycosidic GDGTs, are not suitable as biomarkers for live archaea in the deep biosphere.

1. Introduction

Archaea are globally distributed and play important roles in biogeochemical processes (Offre et al., 2013). The archaeal cell membrane lipids consist mainly of glycerol dibiphytanyl glycerol tetraethers (GDGTs), whose biphytanes contain 0-4 cyclopentane moieties (e.g. GDGT-0 to GDGT-3). Crenarchaeol (Cren) and its isomer (Cren') contain 4 cyclopentane and 1 cyclohexane moieties, which are produced exclusively by Thaumarchaeota (Sinninghe Damsté et al., 2002, 2012). GDGT-based proxy TEX_{86} in surface sediments is significantly correlated with the sea surface temperatures (SST) (Schouten et al., 2002; Zhang and Liu, 2018) and has widely applied to reconstruct the paleo-sea surface temperatures. In living cells, GDGTs are linked to polar headgroups like hexose-phosphohexose (HPH), monohexose (1G) and dihexose (2G) (Fig. A.1) (e.g. Schouten et al., 2008; Pitcher et al., 2010; Elling et al., 2014). The dominance of glycosidic headgroups over phospho headgroups was observed in Thaumarchaeota cultures (Elling et al., 2014, 2015, 2017), water columns (Pitcher et al., 2011; Schouten et al., 2012; Xie et al., 2014; Zhu et al., 2016; Sollai et al., 2019) and marine sediments (e.g. Lipp and Hinrichs, 2009; Lengger et al., 2012a; Evans et al., 2017; Dong et al., 2018). IPL-GDGTs are used as biomarkers for living archaea in sedimentary environments (Biddle et al., 2006; Lipp et al., 2008; Schubotz et al., 2011; Rossel et al., 2011; Xie et al., 2014; Evans et al., 2017; Carr et al., 2017), with the assumption that IPL-GDGTs rapidly degraded away the polar headgroups upon cell death and therefore sedimentary IPL-GDGTs are derived from in situ archaeal production.

However, questions have been raised regarding the origins and

* Corresponding author. Department of Ocean Science and Engineering, Southern University of Science and Technology, Shenzhen, 518055, China.
E-mail address: zhangcl@sustech.edu.cn (C. Zhang).

https://doi.org/10.1016/j.dsr.2019.103107
Received 28 May 2019; Received in revised form 4 September 2019; Accepted 6 September 2019
Available online 09 September 2019
0967-0637/

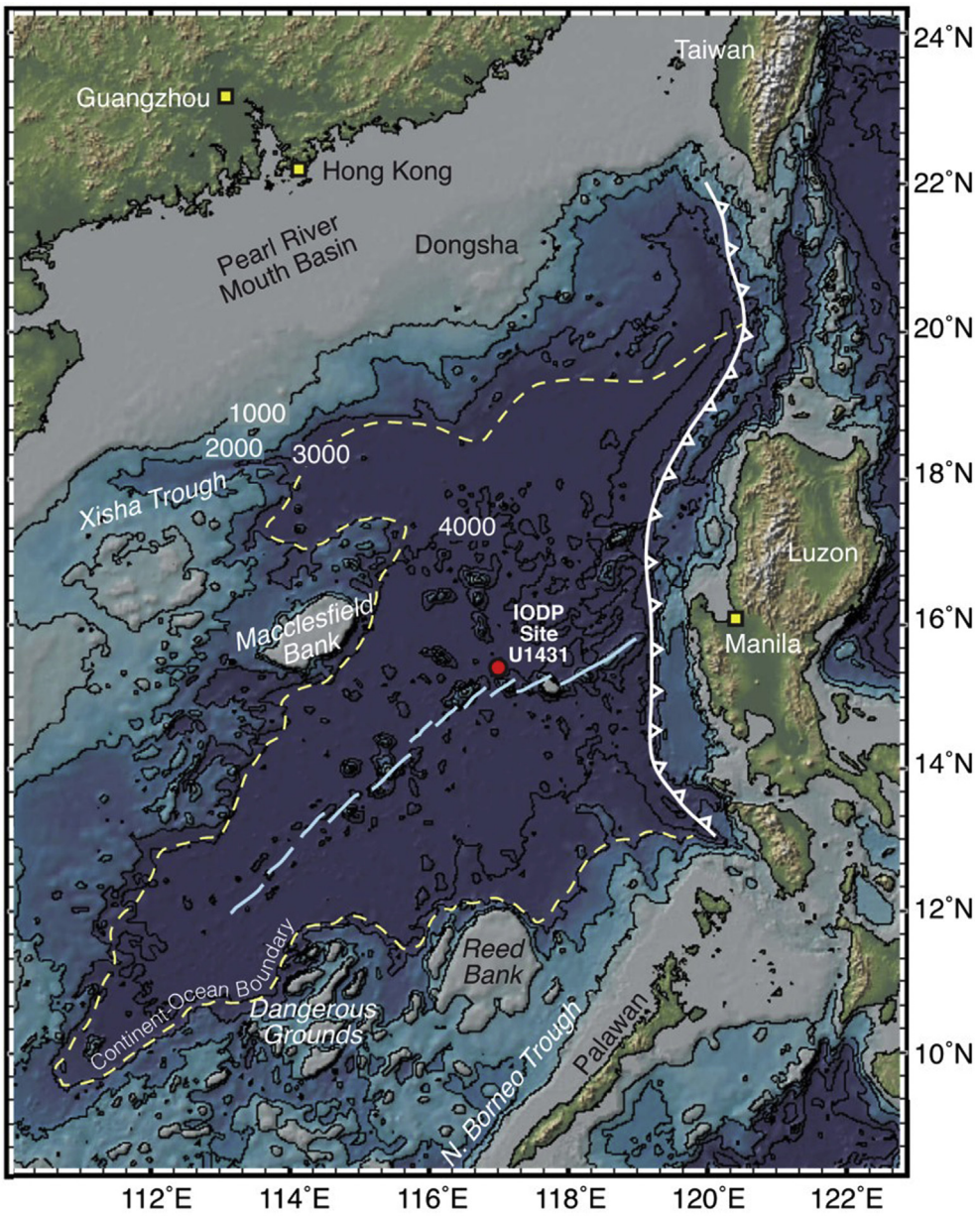

Fig. 1. Site map of IODP U1431 in the SCS.

retardation of IPL-GDGTs' degradation in deeply buried sediments (Lipp and Hinrichs, 2009; Schouten et al., 2010; Lengger et al., 2013, 2014a; Lin et al., 2013; Xie et al., 2013). In marine sediments, the turnover time of extracellular glycosidic IPLs was indicated to reach hundreds of thousands of years (Lin et al., 2013; Xie et al., 2013), which is longer than the microbial turnover time in the deep biosphere (Schippers et al., 2005; Biddle et al., 2006; Lomstein et al., 2012). A degradation model conducted by Schouten et al. (2010) suggested that sedimentary glycosidic GDGTs are derived substantially from the upper water column and can be preserved over geological time scales. Xie et al. (2013) claimed that a substantial portion of archaeal IPLs are accumulative products of past cell generations, highlighting the uncertainty about the source of sedimentary IPL-GDGT pools (Lipp and Hinrichs, 2009; Schouten et al., 2010; Xie et al., 2013). Although some depth profiles of glycosidic GDGTs in marine sediments supported their fossil origins (Lengger et al., 2014b; Dong et al., 2018), the IPL-GDGT profiles over geological time scales are needed for testing this hypothesis based on degradation models. On the other hand, the origin of sedimentary HPH-GDGTs is still illusive, which discounts their potential as biomarkers in the deep biosphere. HPH-GDGTs were detected in shallow sediments from the Arabian Sea and Peru Margin, and attributed to the water column origins (Lengger et al., 2012a, 2014b).

This study investigated the distribution of sedimentary CL and IPL-GDGTs in the context of sediment lithology down to 485 mbsf (~7.3 Ma) from site 1431 of IODP leg 349 in the SCS. The overall results indicated that archaeal lipids in South China Sea sediments bear predominantly signals of a water column origin, which demonstrated differential preservation of different GDGT fractions over geological time scales with HPH-GDGTs most sensitive to degradation.

2. Material and methods

2.1. Site description

Sediments were recovered during the IODP Expedition 349 in the East sub-basin of the SCS at site U1431 (Fig. 1), and spanned the lower Miocene through Pleistocene (Li et al., 2015). The samples investigated were from holes B and D at depths from 0.1 to 485 mbsf (Table A.1).

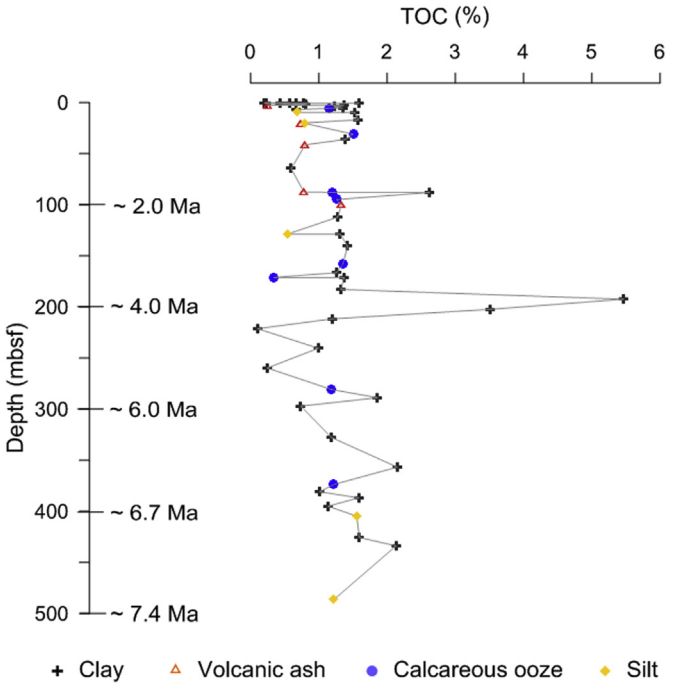

Fig. 2. Total organic carbon content (% organic carbon per g dry weight of sediments) vs. depth (meters below sea floor).

Table 1
Average TOC (%) and average CL, IPL-, 1G- and 2G-GDGT abundances in clay and non-clay sediments (concentration for CL- and IPL-GDGT is in ng per g sediment dry wt, abundance for 1G- and 2G-GDGT is in area per g sediment dry wt).

Lithology	TOC	CL-GDGTs	IPL-GDGTs	2G-GDGTs	1G-GDGTs
Clay (n = 42)	1.3	199.28	19.14	29770	186890
Non-clay (n = 18)	1.0	56.87	6.87	5707	46105

They were stored at −80 °C until analysis. The ages of the sediments were estimated based on reported sedimentation rates of 5 cm ky^{-1} for the upper 0–300 mbsf and ~14 cm ky^{-1} for 300–700 mbsf (Li et al., 2015). The upper 500 m sediments were composed of clay with silt, calcareous ooze and volcanic ash intervals (Li et al., 2015). According to Li et al. (2015), sediment is classified as clay when it contained > 50% clay-sized (particle size < 4 μm) siliciclastic components, and sediment composed of > 50% silt-sized (particle size 4–63 μm) siliciclastic components is called silt. Sediment containing > 50% silt-sized (particle size 4–63 μm) and sand-sized (particle size > 63 μm) primary volcanic grains is classified as volcanic ash. Sediment composed predominantly of calcareous pelagic organisms is classified as calcareous ooze. Lithology was defined based on visual core description, smear slide and thin section inspection, and scanning of an array of physical properties (Li et al., 2015).

2.2. Total organic carbon content

Freeze-dried and ground sediments were analyzed for total organic carbon content (TOC). They were acidified overnight with 2 N HCl, subsequently washed with bidistilled water, and freeze-dried to remove the water. The decalcified samples were measured on a Flash EA 1112 Series (Thermo Scientific, Waltham, MA, USA) analyzer coupled to an HT-Delta V Advantages mass spectrometer. The standard deviation of the replicate measurements was lower than 0.5% for the TOC (n = 5).

2.3. Lipid extraction and separation

Approximately 5–10 g aliquots of freeze-dried and ground sediments were extracted using a modified Bligh-Dyer protocol following Lengger et al. (2012b). The total lipid extracts (TLEs) were stored at −20 °C until analysis. Aliquots of the TLEs were fractionated on a silica column, and separated into the core lipids (CLs) and the intact polar lipids (IPLs) by hexane/ethyl acetate 1:1 (v/v) and MeOH, respectively (Tierney et al., 2012). A C_{46}-GDGT as an internal standard was individually added to the CLs and the IPLs for quantification of GDGTs. One aliquot of the IPLs was converted to CLs by the acidic hydrolysis of the polar head groups, i.e. IPL-derived GDGTs. Hydrolysis of the IPLs was achieved by dissolution in 3 ml of 5% methanolic HCl and heating to 70 °C for 3 h. After being cooled, the solvent was extracted by adding distilled water and DCM, reaching a ratio of 1:1:0.9 (v/v/v, MeOH: DCM: H_2O). The DCM layer was collected and the remaining liquid was washed 3 times with DCM. The total DCM fractions were dried under N_2 gas, yielding IPL-derived GDGTs.

2.4. Analysis of intact polar GDGTs, IPL-derived GDGTs and CL-GDGTs

To investigate the IPL-GDGTs with different polar head groups, aliquots of the TLEs were directly detected by multiple reaction monitoring using reversed phase liquid chromatography and triple quadrupole mass spectrometry equipped with electrospray ionization (RP-LC-ESI-MRM) as described by Chen et al. (2016). Details of HPLC conditions were as described by Zhu et al. (2013). IPL-GDGT components were separated based on the polarity of the headgroups. Absolute quantification of IPLs was not possible due to lacking an internal standard resembling IPL-GDGTs; thus, the response areas per gram dry sediment were calculated and reported (Lengger et al., 2012a, 2014b; 2014c; Evans et al., 2017). The performance of the ESI-MS was monitored by repeat injections of an extract of the Gulf of Mexico surface sediment, typically after 8 sample runs. Relative standard deviations of the areas by five injections were lower than 10%.

Analyses of CL-GDGTs and IPL-derived GDGTs were performed using an HPLC/APCI-MS (Shimadzu LC-MS 8030) following a modified method (Schouten et al., 2007). The detailed conditions of APCI were as described by Wang et al. (2017). Analyses of the CLs, IPLs and hydrolysis IPL fractions showed a nearly complete separation of the CLs and the IPLs over a silicate column: < 0.7% CL-GDGTs were eluted in the IPL fractions. Temperatures were calculated based on the TEX_{86}^{H} calibration (the log of TEX_{86}) according to Kim et al. (2010).

3. Results

TOC ranged from 0.1 to 5.5% without any specific depth trend (Fig. 2, Table A.1). On average, TOC in clay were higher than those in non-clay sediments (Table 1). Concentrations ranged from 0.20 to 204.53 ng g sed dw^{-1} for CL-GDGT-0, 0.19–38.00 ng g sed dw^{-1} for CL-Cren', and 0.12–166.08 ng g sed dw^{-1} for the sum of CL-GDGTs-1, -2 and -3 (Fig. 3A). Individual CL-GDGTs shared common varying trends. This was also observed for the IPL-GDGT pool that had one order of magnitude lower concentrations than CL-GDGTs (Fig. 3B, Table A.1). Total CL- and IPL-GDGT concentrations were still significantly correlated when normalized on TOC ($R^2 = 0.86$, $p < 0.01$) (Fig. A.2). On average, higher concentrations of CL-GDGTs ($t = 2$, $p < 0.05$) and IPL-GDGTs ($t = 2$, $p < 0.05$) were shown in clay than in non-clay sediments (silt, volcanic ash and calcareous ooze) (Table 1).

The polar headgroups including HPH, 2G and 1G (Fig. A.1) were directly measured by RP-LC-ESI-MRM. The HPH-GDGTs peaked at 0.10 mbsf with 5×10^4 area g sed dw^{-1}, rapidly decreased with sediment depth and were below detection limits under ~31 mbsf (Fig. 4, Table A.1). 2G-GDGTs ranged from 10^2 to 10^5 area g sed dw^{-1}, while 1G-GDGTs varied from 10^3 to 10^6 area g sed dw^{-1} (Fig. 4, Table A.1). 2G-GDGTs and 1G-GDGTs showed no specific trend with depth, but

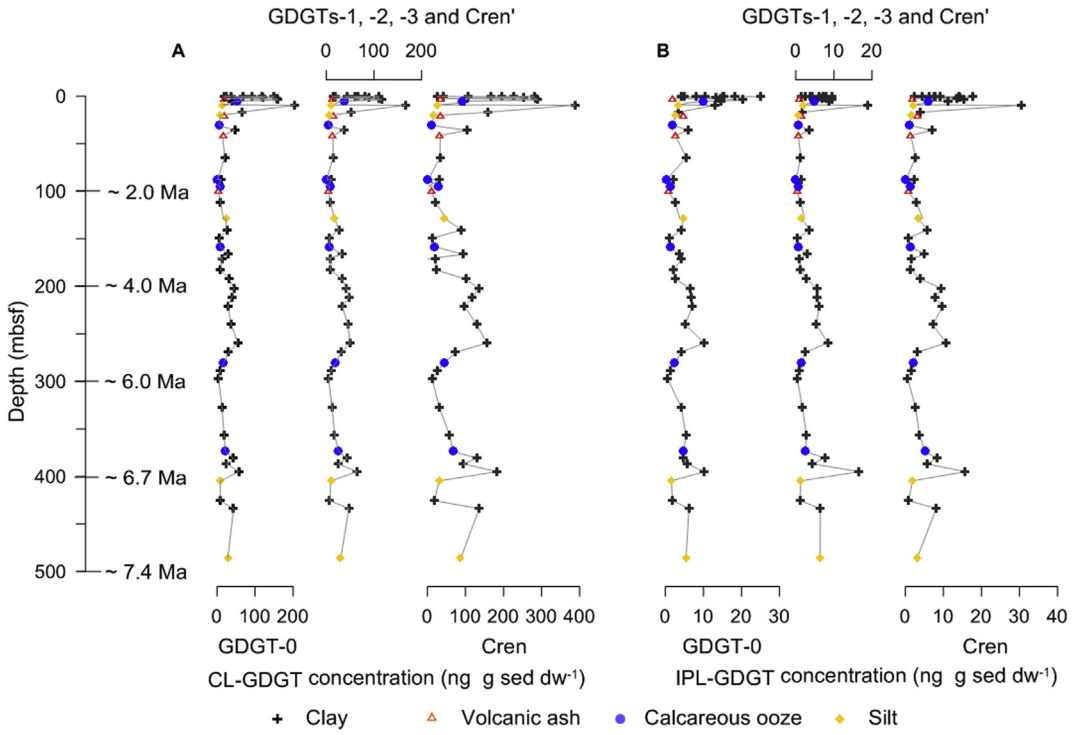

Fig. 3. Depth and lithologic profiles of GDGT concentrations. A) Core-GDGTs. B) IPL-derived GDGTs.

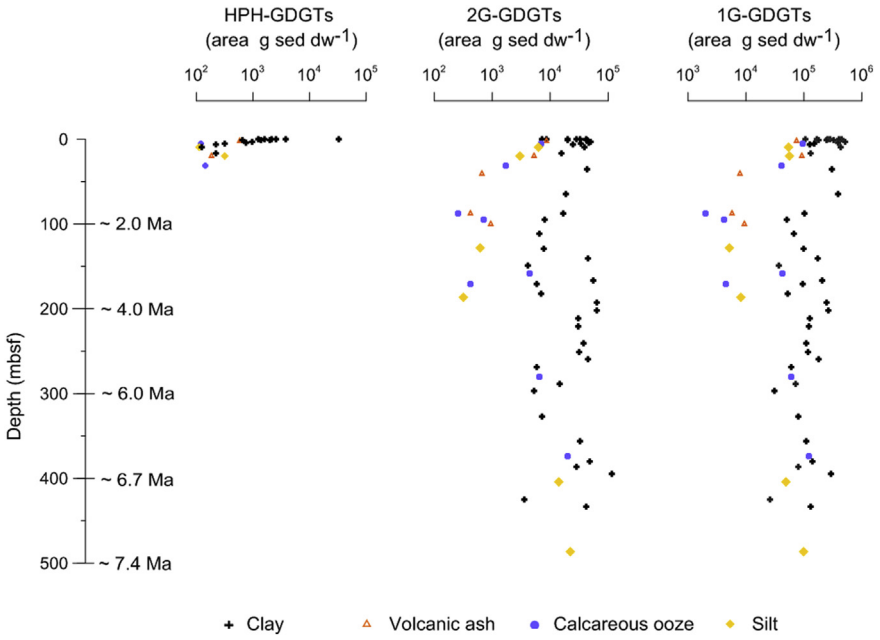

Fig. 4. Depth and lithologic profiles of HPH-, 2G-, and 1G-GDGT abundances.

they had systematically higher abundances in clay than non-clay sediments ($p < 0.01$) (Table 1, Fig. 4). The profiles of IPL-GDGTs with polar head groups showed almost no change when their abundances were normalized on TOC (Fig. A.3).

HPH-GDGTs were dominated by GDGT-0, whose relative abundance was > 56% (Fig. 5, Table A.1). Both 1G-GDGTs and CL-GDGTs consist mainly of GDGT-0 and Cren, while 2G-GDGTs were composed mostly of GDGT-2 and Cren' (Fig. 5, Table A.1). Sedimentary IPL-GDGT compositions were compared with those in water columns and marine thaumarchaeal cultures, they overlapped mostly with the distributional range of data for water columns, and deviated from those of data for marine thaumarchaeal cultures (Fig. 6).

The TEX_{86} derived SST were calculated for CL-, IPL-, 1G- and 2G-GDGTs. CL-TEX_{86} derived SST varied from 23.1 to 28.8 °C, while IPL-TEX_{86} deirved SST exhibited a large range between 22 and 33.3 °C (Fig. 7). 2G-TEX_{86} derived SST were systematically higher than CL-TEX_{86} derived SST, varing between 30.2 and 36.4 °C (Fig. 7). 1G-TEX_{86} derived SST ranged from 18 to 32.6 °C (Fig. 7). The depth profile of 2G-TEX_{86} derived SST paralled those of CL-TEX_{86} derived SST (Fig. 7). CL-TEX_{86} was significantly correlated with 2G-TEX_{86} ($R^2 = 0.63$, $p < 0.01$) and 1G-TEX_{86} ($R^2 = 0.30$, $p < 0.01$) (Fig. A.4).

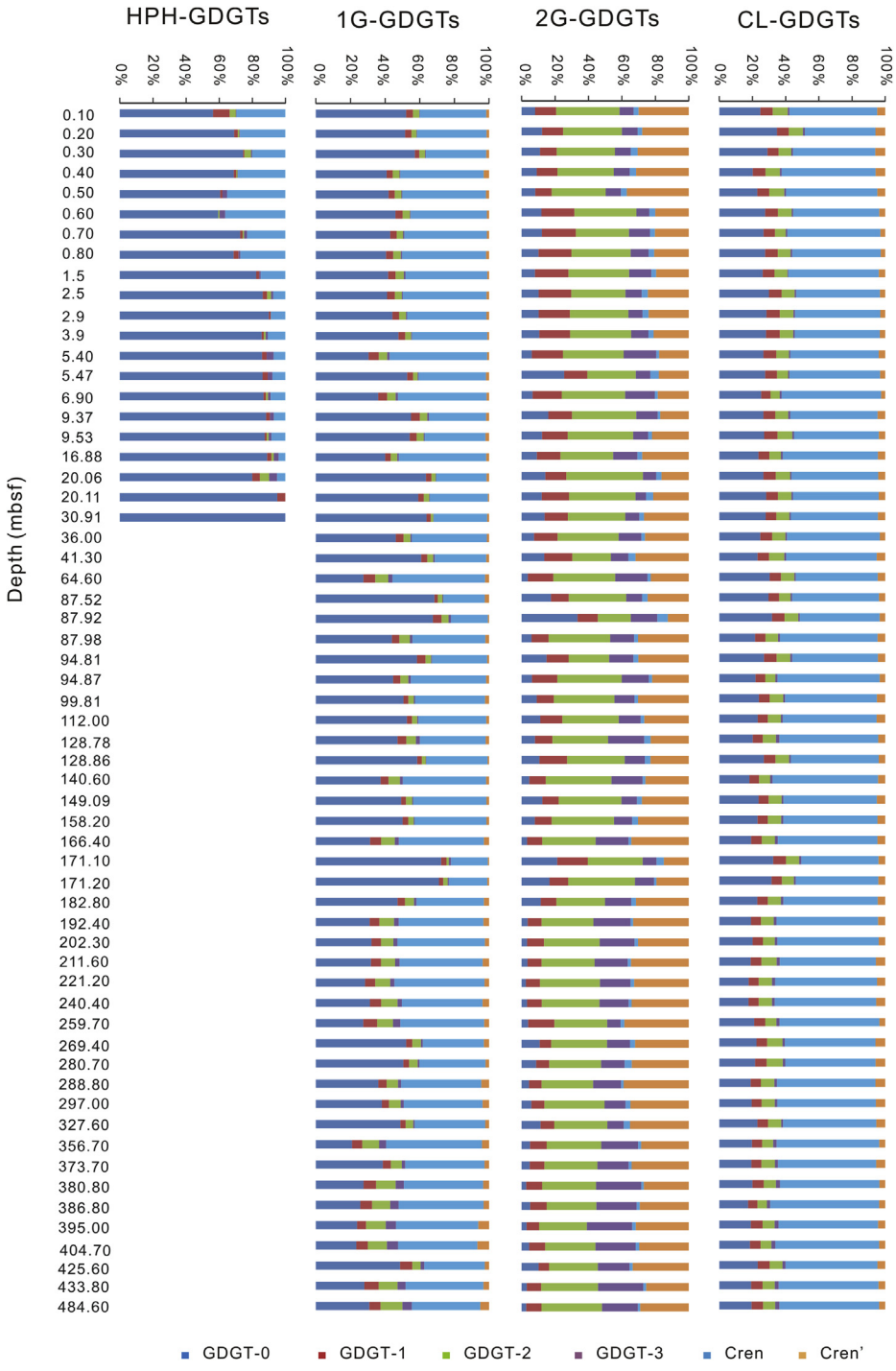

Fig. 5. Variation of HPH-, 2G-, 1G- and CL-GDGT compositions with increasing depth in the core U1431.

4. Discussion

The exact origins of sedimentary IPL-GDGTs are unclear. Degradation models suggested different primary sources of sedimentary IPL-GDGTs from either water columns or sediments (Lipp and Hinrichs et al., 2009; Schouten et al., 2010; Xie et al., 2013), which need to be verified by field data. Our results show that the variation trend of individual CL-GDGT compounds paralled those of IPL-derived GDGTs (Fig. 3), suggesting their shared sources or being determined by similar factors such as TOC. However, total CL- and IPL-derived GDGT concentrations were still significantly correlated ($R^2 = 0.86$, $p < 0.01$) when normalized on TOC (Fig. A.2). The connection between the IPL- and CL-GDGT pools was previously ascribed to the synthesis of IPL-GDGTs via recycling CL-GDGTs by benthic archaea (archaea living in sediments) (Takano et al., 2010; Liu et al., 2011). However, the production rates of glycosidic lipids by marine benthic archaea were rather slow even when labile organic matter was supplied (Lin et al., 2013). Therefore, IPL-GDGTs could share the same origin with CL-GDGTs. Furthermore, CL-TEX_{86} derived SST ranged from 23 to 29 °C, IPL-TEX_{86} deirved SST exhibited a large range between 22 and 33.3 °C (Fig. 7). Both of them were close to the SST (> 20 °C in the SCS), further supporting that sedimentary CL- and IPL-GDGTs are predominantly from the water column.

Direct measurement of IPL-GDGTs with different polar headgroups

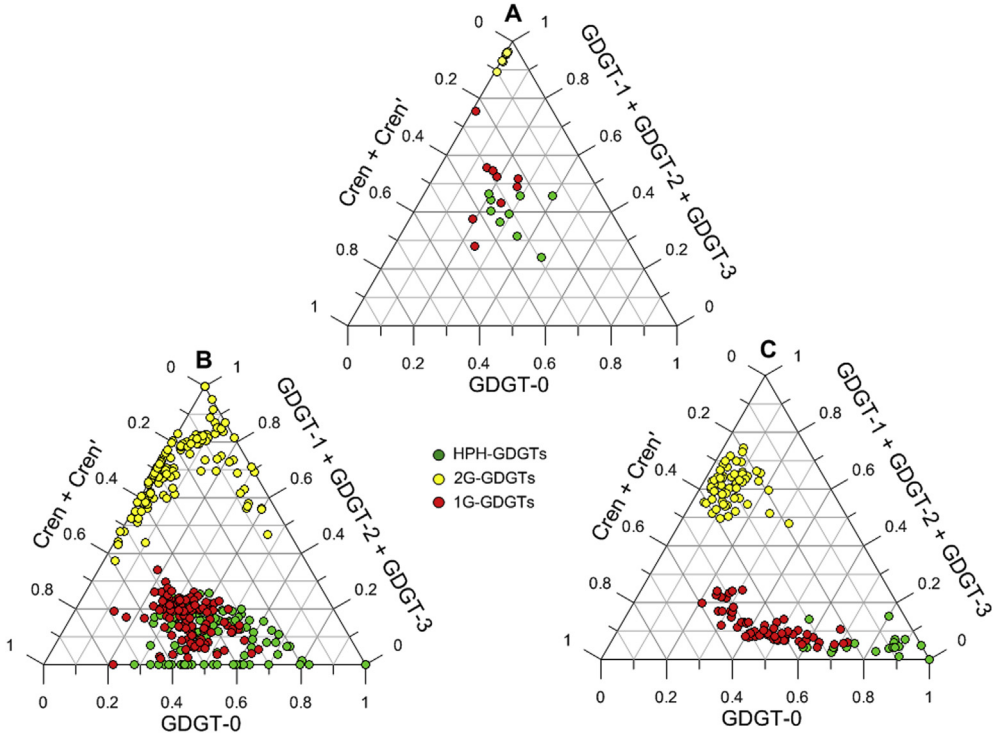

Fig. 6. Ternary diagrams comparing HPH-, 2G- and 1G-GDGT compositions. A) Data for marine Thaumarchaeota cultures from Elling et al. (2014) and Elling et al. (2017). B) Data for water SPM in diverse ocean regimes from Zhu et al. (2016) and Black Sea from Sollai et al. (2019). C) Data for sediments in this study.

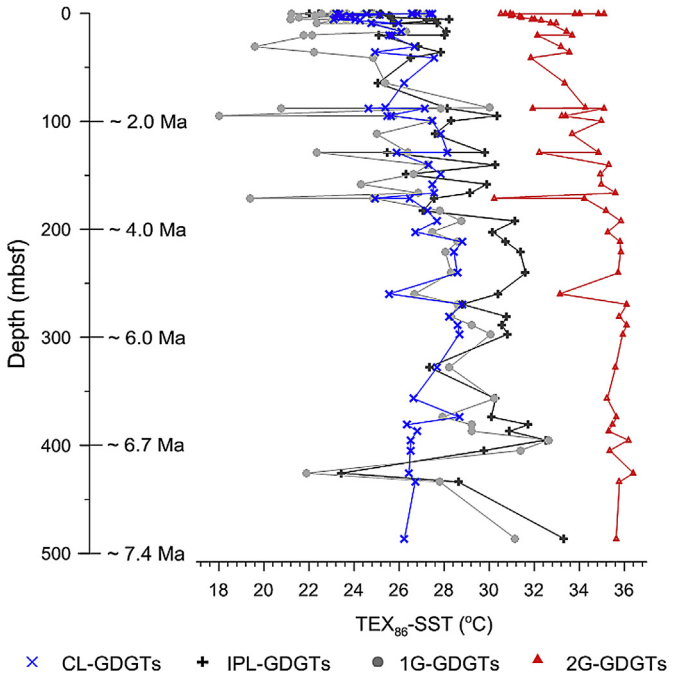

Fig. 7. TEX_{86}-derived SST with changing depth in the core U1431.

allowed us to investigate their origins and degradation behaviours. HPH-GDGTs were mainly composed of GDGT-0 (> 56%), 1G-GDGTs were dominated by GDGT-0 and Cren, and 2G-GDGTs consist primarily of GDGT-2 and Cren' (Fig. 5). The distributions of sedimentary HPH-, 1G-, and 2G-GDGT compositions (Fig. 6C) overlapped with water column data (Zhu et al., 2016; Sollai et al., 2019) (Fig. 6B), suggesting that they could predominantly originate from the water column. In contrast, the sedimentary IPL-GDGT distributions (Fig. 6C) obviously deviated from data for marine thaumarchaeal cultures (Elling et al., 2014, 2017) (Fig. 6A). Since the currently studied cultures do not represent the full diversity of pelagic Thaumarchaeota and there are no cultures of meso/bathypelagic Thaumarchaeota and any Euryarchaeota, it is possible that Thaumarchaeota in the SCS water column have distinct lipid compositions or that pelagic Euryarchaeota may also make significant contributions to the IPL-GDGT pools (Lincoln et al., 2014).

HPH-GDGT abundances decreased rapidly with sediment depth and became undetectable below 31 mbsf (~0.6 Ma). It is in agreement with the results by Lengger et al. (2014b) that HPH-GDGTs fast declined within 6 m sediments in Peru margin, confirming the predictions by Schouten et al. (2010) on the fast disappearance of GDGTs with phosphohexose headgroup. It may be caused by easy degradation of GDGTs with phosphour headgroups. In contrast to HPH-GDGTs, 1G- and 2G-GDGTs dominated the sediments at depth > 31 mbsf (Fig. 4), consistent with other observations (Lipp et al., 2008; Lipp and Hinrichs, 2009; Liu et al., 2011; Lengger et al., 2014b) which found only glycosidic GDGTs in deep sediments. It is likely due to better preservation of GDGTs with glycosdic headgroups compared to GDGTs with phosphate headgroups or due to archaea in deep sediments producing only glycosidic GDGTs. However, the significant contribution by live archaea in sediments to the sedimentary 1G- and 2G-GDGT pools was discarded by two lines of evidence. Firstly, Cren and Cren' has only been detected in Thaumarchaeaota conducting the aerobic oxidation of ammonia and not in anaerobic archaea until now. If living archaea in sediments significantly contributed to glycosidic GDGTs, Cren and Cren' in glycosidic GDGTs would not be expected in the deep sediments where anaerobic archaea inhabit. In fact, Cren or Cren' were still major components in the 1G- and 2G-GDGT pools in deep sediments (Fig. 5). Secondly, SST derived from 1G-TEX_{86} and 2G-TEX_{86} ranged 18–32.6 °C and 30.2–36.4 °C, respectively (Fig. 7), supporting their predominant origins from the water column rather than in situ production that would register a cold seafloor temperature. Interestingly, 1G- and 2G-GDGTs displayed higher abundances in clay than non-clay sediments ($p < 0.01$), similar to CL-GDGT concentrations and TOC (Table 1). This is likely due to their initially higher abundances and/or better preservation in clay than non-

clay sediments.

Our results have implications for the application of IPL-GDGTs as biomarkers for archaea in deeply buried sediments. Sedimentary HPH-, 1G- and 2G-GDGTs are predominantly derived from the water column and therefore are not suitable to represent living archaea in marine deep biosphere. This presents a great challenge for identifying lipid biomarkers exclusively produced by extant sedimentary archaeal communities in the deep marine biosphere.

5. Conclusions

The analysis of the subsurface sediments from the SCS showed the consistent variation patterns of IPL-GDGT concentrations with those of CL-GDGTs. Both CL-and IPL-TEX_{86} derived SST are in the range of the SST in the SCS. Direct measurements of individual IPL-GDGTs with different polar headgroups showed that the compositions of sedimentary HPH-, 2G- and 1G-GDGTs are similar to those in water columns. These results supported the predominant sources of IPL-GDGTs from the water column. HPH-GDGT abundance decreased rapidly to below detection limit at ~31 mbsf while 1G- and 2G-GDGTs dominated the deeply buried sediments, indicating better preservations of glycosidic GDGTs than HPH-GDGTs.

Acknowledgements

Samples were provided by the International Ocean Discovery Program (IODP), JOIDES Resolution, Expedition 349. We are grateful to all the participating crews and scientists for sample recovery. Tommy J. Phelps, Fengfeng Zheng, Yufei Chen and Huangmin Ge are thanked for their comments that helped to improve the manuscript. Funding for this research was provided by the State Key R & D Project of China (Grant No. 2018YFA0605800), the National Natural Science Foundation of China (Grant Nos. 91851210, 41530105 & 41673073), the Key Project of Natural Science Foundation of Guangdong Province, China (Grant No. 2018B030311016), the Shenzhen Key Laboratory of Marine Archaea Geo-Omics, Southern University of Science and Technology, China (Grant No. ZDSYS201802081843490), and the Laboratory for Marine Geology, Qingdao National Laboratory for Marine Science and Technology, China (Grant No. MGQNLMTD201810).

Appendix A. Supplementary data

Supplementary data to this article can be found online at https://doi.org/10.1016/j.dsr.2019.103107.

References

Biddle, J.F., Lipp, J.S., Lever, M.A., Lloyd, K.G., Sørensen, K.B., Erson, R., Fredricks, H.F., Elvert, M., Kelly, T.J., Schrag, D.P., Sogin, M.L., Brenchley, J.E., Teske, A., House, C.H., Hinrichs, K.-U., 2006. Heterotrophic archaea dominate sedimentary subsurface ecosystems off Peru. Proceedings of the National Academy of Sciences of the USA 103, 3846–3851.

Carr, S.A., Schubotz, F., Dunbar, R.B., Mills, C.T., Dias, R., Summons, R.E., Mandernack, K.W., 2017. Acetoclastic Methanosaeta are dominant methanogens in organic-rich Antarctic marine sediments. ISME J. 12, 330–342.

Chen, Y., Zhang, C., Jia, C., Zheng, F., Zhu, C., 2016. Tracking the signals of living archaea: a multiple reaction monitoring (MRM) method for detection of trace amounts of intact polar lipids from the natural environment. Org. Geochem. 97, 1–4.

Dong, L., Jia, G., Li, Q., Li, L., Shi, J., Zhang, C., 2018. Intact polar glycosidic GDGTs in sediments settle from water column as evidenced from downcore sediment records. Chem. Geol. https://doi.org/10.1016/j.chemgeo.2018.09.037.

Elling, F.J., Könneke, M., Lipp, J.S., Becker, K.W., Gagen, E.J., Hinrichs, K.-U., 2014. Effects of growth phase on the membrane lipid composition of the thaumarchaeon Nitrosopumilus maritimus and their implications for archaeal lipid distributions in the marine environment. Geochem. Cosmochim. Acta 141, 579–597.

Elling, F.J., Könneke, M., Mußmann, M., Greve, A., Hinrichs, K.-U., 2015. Influence of temperature, pH, and salinity on membrane lipid composition and TEX_{86} of marine planktonic thaumarchaeal isolates. Geochem. Cosmochim. Acta 171, 238–255.

Elling, F.J., Könneke, M., Nicol, G.W., Stieglmeier, M., Bayer, B., Spieck, E., de la Torre, J.R., Becker, K.W., Thomm, M., Prosser, J.I., Herndl, G.J., Schleper, C., Hinrichs, K.-U., 2017. Chemotaxonomic characterisation of the thaumarchaeal lipidome. Environ. Microbiol. 19, 2681–2700.

Evans, T.W., Wörmer, L., Lever, M.A., Lipp, J.S., Lagostina, L., Lin, Y.S., Hinrichs, K.-U., 2017. Size and composition of subseafloor microbial community in the Benguela upwelling area examined from intact membrane lipid and DNA analysis. Org. Geochem. 111, 86–100.

Kim, J.H., Van der Meer, J., Schouten, S., Helmke, P., Willmott, V., Sangiorgi, F., Koç, N., Hopmans, E.C., Sinninghe Damsté, J.S., 2010. New indices and calibrations derived from the distribution of crenarchaeal isoprenoid tetraether lipids: Implications for past sea surface temperature reconstructions. Geochimica et Cosmochimica Acta 74, 4639–4654.

Lomstein, B.A., Langerhuus, A.T., D'Hondt, S., Jorgensen, B.B., Spivack, A.J., 2012. Endospore abundance, microbial growth and necromass turnover in deep sub-sea-floor sediment. Nature 484, 101–104.

Lengger, S.K., Hopmans, E.C., Reichart, G.-J., Nierop, K.G.J., Sinninghe Damsté, J.S., Schouten, S., 2012a. Intact polar and core glycerol dibiphytanyl glycerol tetraether lipids in the Arabian Sea oxygen minimum zone. Part II: selective preservation and degradation in sediments and consequences for the TEX_{86}. Geochem. Cosmochim. Acta 98, 244–258.

Lengger, S.K., Hopmans, E.C., Sinninghe Damsté, J.S., Schouten, S., 2012b. Comparison of extraction and work up techniques for analysis of core and intact polar tetraether lipids from sedimentary environments. Org. Geochem. 47, 34–40.

Lengger, S.K., Kraaij, M., Baas, M., Tjallingii, R., Stuut, J.-B., Hopmans, E.C., Sinninghe Damsté, J.S., Schouten, S., 2013. Differential degradation of intact polar and core glycerol dialkyl glycerol tetraether lipids upon post-depositional oxidation. Org. Geochem. 65, 83–93.

Lengger, S.K., Lipsewers, Y.A., De Haas, H., Sinninghe Damsté, J.S., Schouten, S., 2014a. Lack of ^{13}C-label incorporation suggests low turnover rates of thaumarchaeal intact polar tetraether lipids in sediments from the Iceland shelf. Biogeosciences 11, 201–216.

Lengger, S.K., Hopmans, E.C., Sinninghe Damsté, J.S., Schouten, S., 2014b. Fossilization and degradation of archaeal intact polar tetraether lipids in deeply buried marine sediments (Peru Margin). Geobiology 12, 212–220.

Lengger, S.K., Hopmans, E.C., Sinninghe Damsté, J.S., Schouten, S., 2014c. Impact of sedimentary degradation and deep water column production on GDGT abundance and distribution in surface sediments in the Arabian Sea: implications for the TEX_{86} paleothermometer. Geochem. Cosmochim. Acta 142, 386–399.

Li, C.-F., Lin, J., Kulhanek, D.K., The expedition 349 scientists, 2015. In: Proceedings of the Integrated Ocean Drilling Program, vol. 349 International Ocean Discovery Program, College Station, TX South China Sea Tectonics. https://doi.org/10.14379/iodp.proc.349.105.2015.

Lin, Y.S., Lipp, J.S., Elvert, M., Holler, T., Hinrichs, K.-U., 2013. Assessing production of the ubiquitous archaeal diglycosyl tetraether lipids in marine subsurface sediment using intramolecular stable isotope probing. Environ. Microbiol. 15, 1634–1646.

Lincoln, S.A., Wai, B., Eppley, J.M., Church, M.J., Summons, R.E., DeLong, E.F., 2014. Planktonic Euryarchaeota are a significant source of archaeal tetraether lipids in the ocean. Proc. Natl. Acad. Sci. 111, 9858–9863.

Lipp, J.S., Morono, Y., Inagaki, F., Hinrichs, K.-U., 2008. Significant contribution of Archaea to extant biomass in marine subsurface sediments. Nature 454, 991–994.

Lipp, J.S., Hinrichs, K.-U., 2009. Structural diversity and fate of intact polar lipids in marine sediments. Geochem. Cosmochim. Acta 73, 6816–6833.

Liu, X., Lipp, J.S., Hinrichs, K.U., 2011. Distribution of intact and core GDGTs in marine sediments. Org. Geochem. 42, 368–375.

Offre, P., Spang, A., Schleper, C., 2013. Archaea in biogeochemical cycles. Annu. Rev. Microbiol. 67, 437–457.

Pitcher, A., Rychlik, N., Hopmans, E.C., Spieck, E., Rijpstra, W.I.C., Ossebaar, J., Schouten, S., Wagner, M., Sinninghe Damsté, J.S., 2010. Crenarchaeol dominates the membrane lipids of *Candidatus* Nitrososphaera gargensis, a thermophilic group I.1b Archaeon. ISME J. 4, 542–552.

Pitcher, A., Villanueva, L., Hopmans, E.C., Schouten, S., Reichart, G.J., Sinninghe Damsté, J.S., 2011a. Niche segregation of ammonia-oxidizing archaea and anammox bacteria in the Arabian Sea oxygen minimum zone. ISME J. 5, 1896–1904.

Rossel, P.E., Elvert, M., Ramette, A., Boetius, A., Hinrichs, K.-U., 2011. Factors controlling the distribution of anaerobic methanotrophic communities in marine environments: evidence from intact polar membrane lipids. Geochem. Cosmochim. Acta 75, 164–184.

Sollai, M., Villanueva, L., Hopmans, E.C., Reichart, G.J., Sinninghe Damsté, J.S., 2019. A combined lipidomic and 16S rRNA gene amplicon sequencing approach reveals archaeal sources of intact polar lipids in the stratified Black Sea water column. Geobiology 17, 91–109.

Schippers, A., Neretin, L.N., Kallmeyer, J., Ferdelman, T.G., Cragg, B.A., Parkes, R.J., Jorgensen, B.B., 2005. Prokaryotic cells of the deep sub-seafloor biosphere identified as living bacteria. Nature 433, 861–864.

Schouten, S., Hopmans, E.C., Schefuß, E., Sinninghe Damsté, J.S., 2002. Distributional variations in marine crenarchaeotal membrane lipids: a new tool for reconstructing ancient sea water temperatures? Earth Planet. Sci. Lett. 204, 265–274.

Schouten, S., Huguet, C., Hopmans, E.C., Kienhuis, M.V., Sinninghe Damsté, J.S., 2007. Analytical methodology for TEX_{86} paleothermometry by high-performance liquid chromatography/atmospheric pressure chemical ionization-mass spectrometry. Anal. Chem. 79, 2940–2944.

Schouten, S., Hopmans, E.C., Baas, M., Boumann, H., Standfest, S., Könneke, M., 2008. Intact membrane lipids of "Candidatus Nitrosopumilus maritimus," a cultivated representative of the cosmopolitan mesophilic group I crenarchaeota. Appl. Environ. Microbiol. 74, 2433–2440.

Schouten, S., Middelburg, J.J., Hopmans, E.C., Sinninghe Damsté, J.S., 2010. Fossilization and degradation of intact polar lipids in deep subsurface sediments: a theoretical approach. Geochem. Cosmochim. Acta 74, 3806–3814.

Schouten, S., Pitcher, A., Hopmans, E.C., Villanueva, L., van Bleijswijk, J., Sinninghe Damsté, J.S., 2012. Intact polar and core glycerol dibiphytanyl glycerol tetraether lipids in the Arabian Sea oxygen minimum zone: I. Selective preservation and degradation in the water column and consequences for the TEX_{86}. Geochem. Cosmochim. Acta 98, 228–243.

Schubotz, F., Lipp, J.S., Elvert, M., Hinrichs, K.-U., 2011. Stable carbon isotopic compositions of intact polar lipids reveal complex carbon flow patterns among hydrocarbon degrading microbial communities at the Chapopote asphalt volcano. Geochem. Cosmochim. Acta 75, 4399–4415.

Sinninghe Damsté, J.S., Schouten, S., Hopmans, E.C., van Duin, A.C.T., Geenevasen, J.A.J., 2002. Crenarchaeol: the characteristic core glycerol dibiphytanyl glycerol tetraether membrane lipid of cosmopolitan pelagic crenarchaeota. JLR (J. Lipid Res.) 43, 1641–1651.

Sinninghe Damsté, J.S., Rijpstra, W.I.C., Hopmans, E.C., Jung, M.Y., Kim, J.G., Rhee, S.K., Stieglmeier, M., Schleper, C., 2012. Intact polar and core dibiphytanyl glycerol tetraether lipids of group I.1a and I. 1b thaumarchaeota in soil. Appl. Environ. Microbiol. 78, 6866–6874.

Takano, Y., Chikaraishi, Y., Ogawa, N.O., Nomaki, H., Morono, Y., Inagaki, F., Kitazato, H., Hinrichs, K.-U., Ohkouchi, N., 2010. Sedimentary membrane lipids recycled by deep-sea benthic archaea. Nat. Geosci. 3, 858–861.

Tierney, J.E., Schouten, S., Pitcher, A., Hopmans, E.C., Sinninghe Damsté, J.S., 2012. Core and intact polar glycerol dialkyl glycerol tetraethers (GDGTs) in Sand Pond, Warwick, Rhode Island (USA): insights into the origin of lacustrine GDGTs. Geochem. Cosmochim. Acta 77, 561–581.

Wang, H., Leng, Q., Liu, W., Yang, H., 2017. A rapid lake-shallowing event terminated preservation of the miocene clarkia fossil konservat-lagerstätte (Idaho, USA). Geology 45, 239–242.

Xie, S., Lipp, J.S., Wegener, G., Ferdelman, T.G., Hinrichs, K.-U., 2013. Turnover of microbial lipids in the deep biosphere and growth of benthic archaeal populations. Proceedings of the National Academy of Sciences of the USA 110, 6010–6014.

Xie, S., Liu, X.-L., Schubotz, F., Wakeham, S.G., Hinrichs, K.-U., 2014. Distribution of glycerol ether lipids in the oxygen minimum zone of the Eastern Tropical North Pacific Ocean. Org. Geochem. 71, 60–71.

Zhang, Y.G., Liu, X., 2018. Export depth of the TEX_{86} signal. Paleoceanography and Paleoclimatology 33, 666–671.

Zhu, C., Lipp, J.S., Wörmer, L., Becker, K.W., Schröder, J., Hinrichs, K.-U., 2013. Comprehensive glycerol ether lipid fingerprints through a novel reversed phase liquid chromatography-mass spectrometry protocol. Org. Geochem. 65, 53–62.

Zhu, C., Wakeham, S.G., Elling, F.J., Basse, A., Mollenhauer, G., Versteegh, G.J., Hinrichs, K.-U., 2016. Stratification of archaeal membrane lipids in the ocean and implications for adaptation and chemotaxonomy of planktonic archaea. Environ. Microbiol. 18, 4324–4336.